

Review

Ins and Outs of the Ankle Syndesmosis from a 2D to 3D CT Perspective

Thibaut Dhont ^{1,†}, Manu Huyghe ^{1,†}, Matthias Peiffer ^{2,*} , Noortje Hagemeijer ³, Bedri Karaismailoglu ^{4,5} , Nicola Krahenbuhl ⁶, Emmanuel Audenaert ² and Arne Burssens ² 

¹ Faculty of Medicine and Health Sciences, Ghent University, 9000 Gent, Belgium

² Department of Orthopedic Surgery and Traumatology, Ghent University Hospital, 9000 Ghent, Belgium

³ Department of Orthopedic Surgery, Amsterdam UMC, University of Amsterdam, Meibergdreef 9, 1105 AZ Amsterdam, The Netherlands

⁴ Department of Orthopedics and Traumatology, Istanbul University-Cerrahpasa, 34320 Istanbul, Turkey

⁵ CAST-Cerrahpasa Research, Simulation and Design Laboratory, Istanbul University-Cerrahpasa, 34320 Istanbul, Turkey

⁶ Department of Orthopedics and Traumatology, Universitätsspital Basel, 4031 Basel, Switzerland

* Correspondence: matthias.peiffer@ugent.be; Tel.: +32-9332-2251

† These authors contributed equally to this work.

Abstract: Despite various proposed measurement techniques for assessing syndesmosis integrity, a standardized protocol is lacking, and the existing literature reports inconsistent findings regarding normal and abnormal relationships between the fibula and tibia at the distal level. Therefore, this study aims to present an overview of two- (2D) and three-dimensional (3D) measurement methods utilized to evaluate syndesmosis integrity. A topical literature review was conducted, including studies employing 2D or 3D measurement techniques to quantify distal tibiofibular syndesmosis alignment on computed tomography (CT) or weight-bearing CT (WBCT) scans. A total of 49 eligible articles were included in this review. While most interclass correlation (ICC) values indicate favorable reliability, certain measurements involving multiple steps exhibited lower ICC values, potentially due to the learning curve associated with their implementation. Inconclusive results were obtained regarding the influence of age, sex, and height on syndesmotomic measurements. No significant difference was observed between bilateral ankles, permitting the use of the opposite side as an internal control for comparison. There is a notable range of normal and pathological values, as evidenced by the standard deviation associated with each measurement. This review highlights the absence of a consensus on syndesmotomic measurements for assessing integrity despite numerous CT scan studies. The diverse measurement techniques, complexity, and inconclusive findings present challenges in distinguishing between normal and pathological values in routine clinical practice. Promising advancements in novel 3D techniques offer potential for automated measurements and reduction of observer inaccuracies, but further validation is needed.

Keywords: ankle syndesmosis; weightbearing CT; 3D modelling; 2D measurements; sport injuries



Citation: Dhont, T.; Huyghe, M.; Peiffer, M.; Hagemeijer, N.; Karaismailoglu, B.; Krahenbuhl, N.; Audenaert, E.; Burssens, A. Ins and Outs of the Ankle Syndesmosis from a 2D to 3D CT Perspective. *Appl. Sci.* **2023**, *13*, 10624. <https://doi.org/10.3390/app131910624>

Academic Editor: Matej Supej

Received: 24 July 2023

Revised: 13 September 2023

Accepted: 21 September 2023

Published: 23 September 2023



Copyright: © 2023 by the authors. Licensee MDPI, Basel, Switzerland. This article is an open access article distributed under the terms and conditions of the Creative Commons Attribution (CC BY) license (<https://creativecommons.org/licenses/by/4.0/>).

1. Introduction

The ankle syndesmosis entails a complex interplay of bony and ligamentous structures. The ankle ligaments play a crucial role in preventing tibiofibular displacement and maintaining a stable ankle mortise [1]. When this syndesmotomic complex is impaired due to injury, whether high ankle sprains or fracture-associated, the normal mortise configuration is disrupted, leading to atypical biomechanics of the tibiotalar joint. This can result in an alteration of the contact area between the tibia and talus, leading to heightened pressure on the talar dome and tibial plafond [1,2]. The syndesmosis is injured in 4–24% of all ankle sprains and 10–45% of cases with concomitant ankle fractures [3–6]. Subgroups with more

risk include athletes, females, children, adolescents, and patients with a history of ankle sprains [7].

The diagnosis of syndesmotic injuries is crucial as untreated or misdiagnosed lesions can lead to irreversible, long-term morbidity such as pain, poor function, mortise incongruence, early osteoarthritis, anterolateral soft tissue impingement, and local synovitis [4,8–10]. An accurate diagnosis can be obscured due to the low sensitivity and specificity of the clinical examination tests (i.e., ligament palpation tenderness, external rotation stress test according to Frick, squeeze test, cotton test, and fibula translation test) [11,12]. Consequently, advanced imaging modalities such as computed tomography (CT), magnetic resonance imaging (MRI), or arthroscopy are indispensable in current clinical practice [3,13,14]. Although arthroscopy is the most reliable method for diagnosis, it is hampered by its invasive nature, cost, and lack of native contralateral reference [9,10,13,14]. Therefore, non-invasive imaging modalities have been broadly described to visualize the syndesmosis and detect injury. However, their true value in diagnosing instability and integrity remains equivocal [8,14,15]. Radiographs are poorly sensitive and may be valuable only in cases of severe instability [8,9]. Furthermore, the position of the hindfoot during radiography affects the measurements subsequently [16]. Supine CT, on the other hand, has improved levels of sensitivity, but it underestimates the extent of subtle lesions due to its non-weight-bearing and non-dynamic nature [3,10]. While MRI is highly accurate in identifying ligamentous damage, its availability may be limited, and even when it detects such injury, it does not necessarily indicate the presence of instability [17,18]. Meanwhile, weight-bearing CT (WBCT) provides less radiation and allows for three-dimensional (3D) imaging of the weight-bearing dynamism, with the contralateral ankle serving as an internal control given the variable anatomy of the incisura [3,8,10].

Although several measurement techniques have been proposed to assess the syndesmosis, there is no established protocol, and the available literature shows inconsistent findings regarding the range of (ab)normal relationships between the fibula and tibia at the distal level. Therefore, the aim of this study is to provide an overview of the two-dimensional (2D) and 3D measurement methods for evaluating the integrity of the syndesmosis.

2. Methodology

2.1. Search Strategy

A topical literature review was conducted. Three major medical databases (PubMed, Web of Science, and Google Scholar) were searched through June 2023. The following search terms were used: (syndesmosis injury OR distal tibiofibular joint injury OR syndesmotic injury OR syndesmosis instability OR syndesmotic instability OR distal tibiofibular joint instability) and (CT OR computed tomography OR WBCT OR weight-bearing CT OR weight-bearing computed tomography). No limitations were held on the type of journal or publication date of the article.

2.2. Study Selection

The records were screened independently by two reviewers (T.D. and M.H.). Inclusion criteria were composed of studies involving 2D or 3D measurement methods to quantify the alignment of the distal tibiofibular syndesmosis on CT and WBCT imaging. Exclusion criteria consisted of case reports, review articles, different imaging modalities (i.e., ultrasound, MRI, or arthroscopy), studies involving patients < 18 years old, studies concerning post-operative alignment, and manuscripts in languages other than English. The additional literature was obtained by searching references in the manuscripts (“snowball method”) [19].

2.3. Data Extraction

Mean values, normative reference values, pathological values, and interobserver reliability values (ICC) for the measurement methods were extracted from every record, if avail-

able. The weighted mean and standard deviation were calculated for every measurement method included in each record. The normative reference limit for these measurements was extracted, and the weighted mean was calculated if more than two reference limits were available for one measurement. Since weight-bearing has been reported to affect the kinematics of the syndesmosis [20], mean and reference values were established separately for WBCT and conventional CT studies. All calculations were computed using Microsoft® Excel (version 1808, 2019).

3. Results

3.1. Search Results

The aforementioned literature search generated 1716 articles. After the removal of duplicates, 1249 records remained and were consequently screened on the title, after which 262 were suitable for abstract assessment. After reviewing the abstracts, 53 articles met the inclusion criteria. The researchers assessed the final 53 records for eligibility. A total of 13 records were excluded based on the following criteria: case reports ($n = 2$), review articles ($n = 3$), other imaging modalities ($n = 6$), and studies including patients < 18 years old ($n = 2$). Moreover, nine additional studies were identified through the references cited in the selected manuscripts. Finally, 49 articles were included in the review (Figure 1).

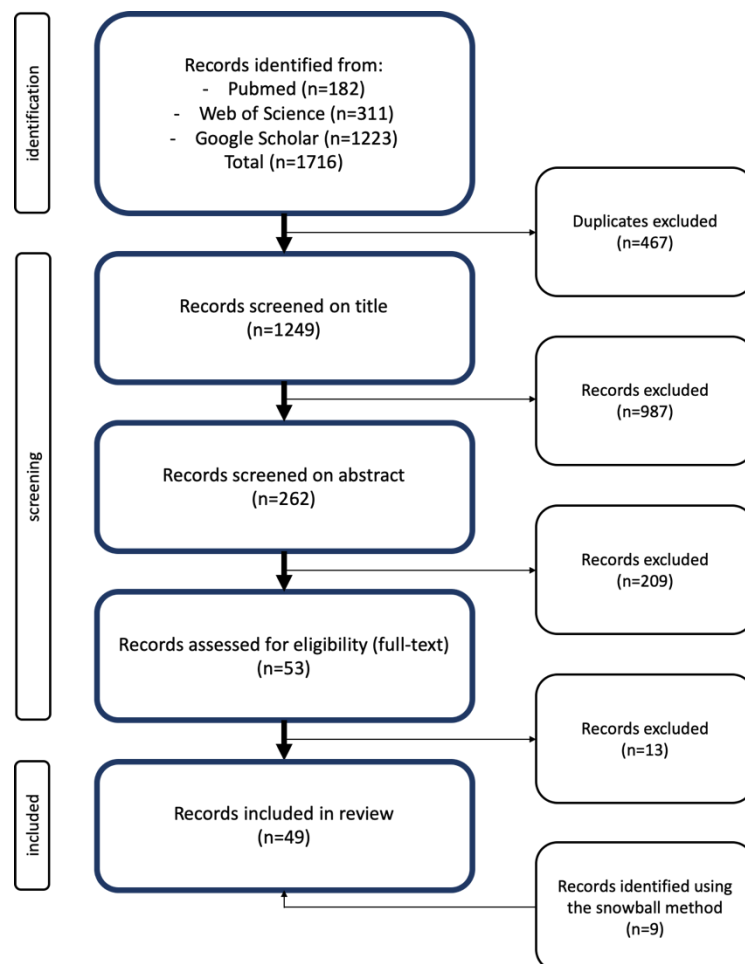


Figure 1. Flowchart illustrating the selection process of the included articles, according to the PRISMA guidelines [21].

3.2. Study Characteristics

Data were extracted from 29 of the 49 trials. The other trials were used to describe the measurements and their usefulness in daily practice but did not provide useful data.

Out of these, 13 (45%) articles utilized CT to assess the integrity of the syndesmosis, while 10 (35%) articles used WBCT, and 6 (20%) articles employed both methods. Furthermore, 8 studies analyzed both injured and healthy patients, while 1 study focused solely on injured patients, and 11 studies exclusively examined healthy individuals. Moreover, 1 article conducted its examination on cadaveric populations, whereas 19 articles conducted their examinations on in vivo populations. Additionally, out of the 13 measurements discussed in this review, only 1 measurement was performed at the talocrural level instead of 1 cm proximal to the tibia plafond. Ten articles were focused on novel (3D) imaging techniques.

3.3. Conventional 2D Measurements

In Table 1, a description of all 2D measurements is provided. Table 2 presents the mean, normative reference limit, and ICC per measurement, if available. Figures 2–4 depict the mediolateral translation measurements, fibular rotation measurements, and fibular translation measurements, respectively.

Table 1. Description of radiological measurements.

Measurement	Description	References
a. Mediolateral translation (diastasis)		
Anterior tibiofibular width (A)	The distance between the anterior tibial tubercle and the nearest fibular point.	[5,6,13,18,20,22–32]
Posterior tibiofibular width (B)	The distance between the posterior tibial tubercle and the nearest fibular point.	[5,6,13,20,22–24,26–29,31,32]
Middle tibiofibular width	The distance between the most central point of the incisura and the nearest fibular point.	[5,13,18,20,28,31–33]
Maximum tibiofibular width	The maximal distance between the tibia and fibula, regardless of the location	[32]
Minimum tibiofibular width	The minimal distance between the tibia and fibula, regardless of the location.	[26]
Syndesmotic area	The surface area, delineated by the medial cortex of the fibula and the lateral cortex of the tibial incisura, and two lines tangential to the anterior and posterior cortices of the tibia and fibula	[13,26,31,33–35]
b. Fibular rotation		
Fibular rotation by Dikos (α)	The angle between the fibular axis and the tangential line to the anterior and posterior tibial tubercles. A higher angle value indicates internal rotation of the fibula, while a lower angle value indicates external rotation.	[5,13,20,22,26,28,29,31,33,36]
Tang ratio	The ratio of distances from the tibial centroid to the most anterior fibular point and from the tibial centroid to the most posterior fibular point.	[23,26,29]
Ratio A/B	The ratio between the anterior tibiofibular width (A) and posterior tibiofibular width (B). The ratio increases as the fibula externally rotates.	[5,20,28]
Bimalleolar angle (β)	The angle between the tangential line to the medial cortex of the lateral malleolus and the tangential line to the lateral cortex of the medial malleolus, at the level of the talar dome or more distally.	[28,37]

Table 1. *Cont.*

Measurement	Description	References
c. Fibular translation		
Anteroposterior translational ratio by Nault	This is a three-step measurement. A line is drawn between the most anterior and most posterior points of the incisura. A perpendicular line is drawn in the middle of the first line. The distance between the anterior part of the fibula and the perpendicular line is the distance A. B is the distance between the posterior part of the fibula and the perpendicular line. The ratio A/B represents a description of the anteroposterior position.	[5,20,28]
Medial Phisitkul	A first reference line is established by drawing a tangential line along the most lateral aspect of the anterior and posterior tubercles of the fibular incisura. A second reference line is drawn perpendicular to this line at the anterior tubercle. The distance from the most medial point of the fibula to the first line represents the mediolateral position of the fibula. This measurement is positive if the fibula is lateral to the reference line and negative if the fibula is medial to the reference line.	[23,29,38]
Anterior Phisitkul	This distance is measured from the most anterior point of the fibula to the second reference line explained in the measurement above. If the fibula is anterior to the reference line, the value is negative; if the fibula is posterior to the reference line, the value is positive.	[5,13,20,23,26,28,29,38,39]

Table 2. Mean, definitive normative reference limit, and mean ICC per measurement.

Measurement	Mean ± SD	Definitive Normative Reference Limit	Mean ICC
a. Mediolateral translation (diastasis)			
Anterior tibiofibular width (in mm)	CT, normal: 2.71 ± 0.80 CT, injury: 3.50 ± 1.18 WBCT, normal: 3.51 ± 0.60 WBCT, injury: 3.77 ± 1.1	Cut-off max value, CT: 4 [32] Max normal difference with respect to contralateral ankle, CT: 0.7 [18]	CT: 0.834 WBCT: 0.758
Posterior tibiofibular width (in mm)	CT, normal: 4.74 ± 1.74 CT, injury: 4.92 ± 0.29 WBCT, normal: 5.97 ± 1.48 WBCT, injury: 7.38 ± 2.69	/	CT: 0.799 WBCT: 0.714
Middle tibiofibular width (in mm)	CT, normal: 3.58 ± 0.47 CT, injury: 4.25 ± 1.48 WBCT, normal: 4.28 ± 0.78 WBCT, injury: 5.05 ± 1.34	Cut-off max value, CT: 3.95 [32] Cut-off for the difference between injured and uninjured ankle, CT: 1.7 [18] Normative reference range, WBCT: 1.23–5.2 [5]	CT: 0.788 WBCT: 0.803
Maximum tibiofibular width (in mm)	CT, normal: 4.6 ± 1.4 CT, injury: 7.2 ± 2.96 WBCT, normal: / WBCT, injury: /	Cut-off max value, CT: 5.65 [32]	CT: 0.865
Minimum tibiofibular width (in mm)	CT, normal: 1.6 ± 0.2 CT, injury: 2.9 ± 0.3 WBCT, normal: 2.6 ± 0.2 WBCT, injury: 2.9 ± 0.3	/	CT: 0.899 WBCT: 0.875

Table 2. Cont.

Measurement	Mean \pm SD	Definitive Normative Reference Limit	Mean ICC
Syndesmotic area (in mm ²)	CT, normal: 105.2 \pm 22.6 CT, injury: 129.5 \pm 31.3	/	CT: 0.96 WBCT: 0.93
	WBCT, normal: 106.0 \pm 16.9 WBCT, injury: 134.1 \pm 28.2		
b. Fibular rotation			
Fibular rotation Dikos (in degrees)	CT, normal: 13.6 \pm 3.3 CT, injury: 15 \pm 6.4	/	CT: 0.689 WBCT: 0.783
	WBCT, normal: 12.3 \pm 1.8 WBCT, injury: 7.39 \pm 1.1		
Tang ratio	CT, normal: 0.85 \pm 0.05 CT, injury: /	/	CT: 0.47 WBCT: 0.72
	WBCT, normal: 0.85 \pm 0.05 WBCT, injury: /		
Ratio A/B	CT, normal: 0.55 \pm 0.03 CT, injury: /	Normative reference range, WBCT: 0.12–1.08 [5]	CT: 0.722 WBCT: 0.79
	WBCT, normal: 0.62 \pm 0.03 WBCT, injury: /		
Bimalleolar angle (in degrees)	CT, normal: 7.67 \pm 1.1 CT, injury: /	/	CT: 0.68 WBCT: /
	WBCT, normal: / WBCT, injury: /		
c. Fibular translation			
Anteroposterior translational ratio by Nault	CT, normal: 1.54 \pm 0.08 CT, injury: /	Normative reference range, WBCT: 0.31–2.59 [5]	CT: 0.441 WBCT: 0.72
	WBCT, normal: 1.45 \pm 0.00 WBCT, injury: /		
Medial Phisitkul (in mm)	/	/	CT: 0.86
Anterior Phisitkul (in mm)	CT, normal: 1.59 \pm 0.50 CT, injury: 1.79 \pm 1.55	Normative reference range, WBCT: –1.48–3.44 [5]	CT: 0.725 WBCT: 0.763
	WBCT, normal: 1.60 \pm 0.14 WBCT, injury: 1.37 \pm 0.27		

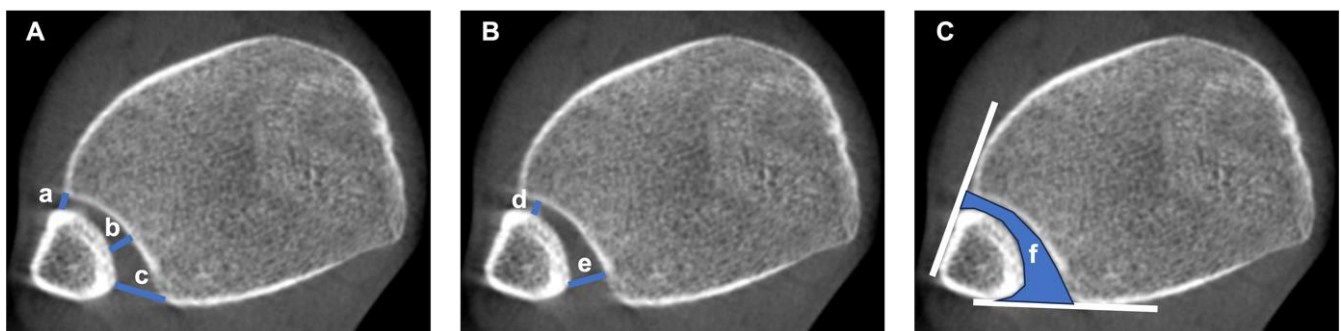


Figure 2. Mediolateral translation measurements on an axial CT image of an uninjured syndesmosis. (A) Anterior tibiofibular width (a), middle tibiofibular width (b), and posterior tibiofibular width (c). (B) Minimum tibiofibular width (d) and maximum tibiofibular width (e). (C) Syndesmotic area (blue area, f), based on the two lines tangential to the anterior and posterior cortices of the tibia and fibula (solid white lines).

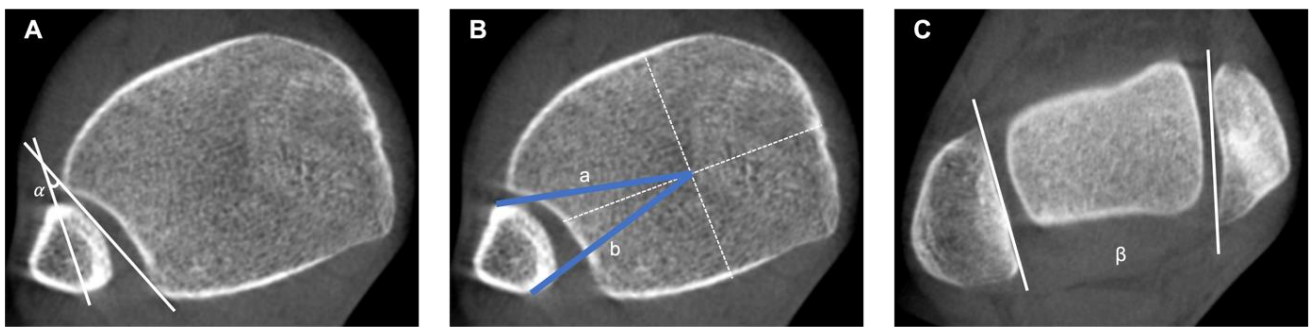


Figure 3. Fibular rotation measurements on an axial CT image of an uninjured syndesmosis and ankle. **(A)** Fibular rotation angle (α) by Dikos, The angle between the fibular axis and the tangential line to the anterior and posterior tibial tubercles (white lines) [36]. **(B)** Tang ratio of anterior (a) and posterior measurement (b), represented as the ratio of distances from the tibial centroid (white dashed lines) to the most anterior fibular point and the most posterior fibular point, respectively (blue solid lines). **(C)** Bimalleolar angle (β), calculated between the tangential line to the medial cortex of the lateral malleolus and the tangential line to the lateral cortex of the medial malleolus (solid white lines).

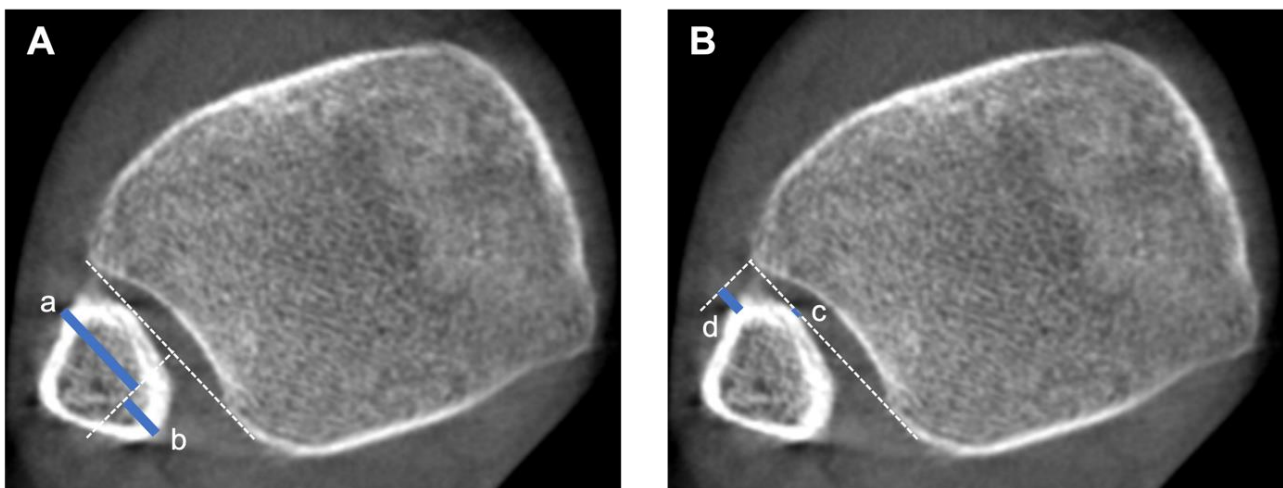


Figure 4. Fibular translation measurements on an axial CT image of an uninjured syndesmosis. **(A)** Anteroposterior translation ratio by Nault [28] of anterior distance (a) and posterior distance (b) (blue lines), calculated based from a perpendicular line, drawn from the middle of a line connecting the most anterior and posterior points of the incisura (white solid lines). **(B)** Medial (c) and anterior (d) Phisitkul measurement (blue lines), calculated from a line connecting the most anterior and posterior points of the incisura, and a perpendicular line perpendicular to the previous line at the level of the anterior tubercle (white dashed lines).

3.3.1. 2D Measurements Quantifying Tibiofibular Translation Mediolateral Translation (Diastasis)

- Anterior, middle, posterior, maximum, and minimum tibiofibular width

First described by Gardner et al. [25], the anterior tibiofibular width (ATFW) and posterior tibiofibular width (PTFW) are the most commonly used measurements of the distal tibiofibular joint in the literature [5,6,13,18,20,22–32]. They serve as indicators of diastasis between the tibia and fibula [29]. Nault et al. introduced the middle tibiofibular width (MTFW) as an additional measurement for diastasis [28]. More recently, Yeung et al. and Ahn et al. introduced the maximum tibiofibular width (MxTFW) and minimum tibiofibular width (MnTFW), respectively [22,32]. These measurements are generally performed at the level of 1 cm proximal to the tibial plafond on axial images, as depicted in Figure 2A,B and

described in Table 1 This level is consistently selected due to the prominent tibial tubercles and well-defined fibular incisura at this extent [6,13,22,24,25,27,28]. Most studies exhibit a wide standard deviation (SD), resulting in a broad normative range [28]. Furthermore, the reference values do not account for age and gender. Park et al. reported that the posterior width is significantly smaller in women ($p < 0.001$), and both ATFW and PTFW significantly decrease with age ($p < 0.001$) [6]. On the other hand, some studies showed no significant difference in AFTW and PFTW by age and gender [29,31]. However, there is no significant difference compared to the contralateral ankle, enabling bilateral comparison in the evaluation of syndesmotic injury [6,31]. No significant differences were observed in the ATFW, PTFW, and MTFW under both normal and weight-bearing conditions. [20,29]. Additionally, the interobserver reliability is excellent for the MnTFW and MxTFW and good for the ATFW, PTFW, and MTFW, indicating the reliability of these parameters.

A recent study compared the ATFW and MTFW of the injured ankle with the contralateral uninjured ankle in 68 patients under non-weight-bearing conditions [18]. The mean distances were 0.3 greater in injured ankles compared to uninjured for both measurements. Ideal cut-off values for instability assessing the difference between the injured and uninjured ankle were set at 0.7 and 1.7 for ATFW and MTFW, respectively. These values demonstrate low sensitivity (25%) but high specificity (97%) for ATFW. For MTFW, the value is primarily useful for ruling out syndesmotic injuries, with low sensitivity (0%) but high specificity (100%) [18]. Another study compared ATFW, MTFW, PTFW, and MxTFW in ankles that were assessed intraoperatively. The ankles were operated on due to ankle fractures, with syndesmotic integrity tests performed to differentiate between stable and unstable syndesmosis. There was a significant difference between the measurements for stable and unstable ankles for the ATFW, MTFW, PTFW, and MxTFW ($p < 0.001$; $p = 0.014$; $p = 0.042$; $p < 0.001$). Cut-off values were set at 4 (sens = 56.5, spec = 91.7) for ATFW, 3.95 (sens = 74.4, spec = 75) for MTFW, and 5.65 (sens = 74.4, spec = 78.9) for MxTFW. The authors recommended that the PTFW should not be used for diagnosis [32]. Hamard et al. conducted non-weight-bearing CT and WBCT scans on injured and uninjured ankles. The distance was significantly greater for the PTFW and MnTFW in both conditions, while the ATFW was only significantly larger in non-weight-bearing conditions [26]. Another study confirmed these findings specifically for ATFW and PTFW in non-weight-bearing conditions [22]. Under weight-bearing conditions, the MTFW is significantly greater in injured ankles [33].

Anteroposterior Translation

- Anteroposterior translation ratio by Nault

This ratio, first described by Nault et al., is a description of the anteroposterior position of the fibula in relation to the incisura and determines translation [28]. This ratio is obtained in three steps, as depicted in Figure 4A and described in Table 1. Due to the complexity of this measurement, the ICC varies in every study. Interestingly, more recent studies have better interobserver reliability than older studies, which could be explained by the learning curve of clinicians [5,20,28].

This measurement has only been documented in uninjured ankles [5,20,28]. In weight-bearing conditions, this ratio is significantly lower ($p = 0.007$) [20]. Injury may be suspected if values are outside the range of 0.31 to 2.59. No sensitivity or specificity is given for this range [5]. As no pathological values are known, these values cannot be compared with pathological values.

- Anterior and Medial Phisitkul

First described by Phisitkul et al., this translational parameter of the fibula has been used to assess syndesmosis reduction following ankle injury. Both measurements are depicted in Figure 4B and described in Table 1 [38]. Nowadays, the anterior Phisitkul is the most commonly used translational measurement [5,13,20,23,26,28,29,38,39].

Interobserver reliability is good for the anterior measurement and excellent for the medial measurement. No mean values could be obtained for the medial measurement.

Conflicting results have been found for differences between the sexes [5,29]. There is no significant difference between the two legs under normal conditions, indicating that the legs can be compared when assessing syndesmotic injury. Moreover, age has no influence on this measurement [5]. Weight-bearing conditions do not exert a substantial influence on both healthy and injured ankles [20]. The area under curve (AUC) values were 0.894 and 0.467 for CT and WBCT, respectively. Therefore, the authors stated that the anterior Phisitkul was excellent at differentiating between normal and injured syndesmosis using non-weight-bearing CT but less reliable in WBCT [26]. A normative reference range of -1.48 to 3.44 was obtained, but no sensitivity or specificity was reported [5].

3.3.1.3. The 2D Measurements Quantifying Tibiofibular Rotation

Assessment of fibular rotation plays a crucial role in evaluating the integrity of the syndesmotic joint. Injuries are generally characterized by diastasis and external rotation of the fibula [3,37]. The most cited method was initially described by Dikos et al., measuring fibular rotation relative to the tibial incisura, 1 cm proximal to the tibial plafond [5,13,20,22,26,28,29,31,33,36]. Alternative measurements are performed at the level of the talar dome or slightly distal therefrom, determining rotation along the medial and lateral malleolus [28,37]. However, some studies do not quantify rotation in degrees but rather use ratios, whereby an increase correlates with the external rotation of the fibula, e.g., the ratio of ATFW and PTFW [5,20,28]. An additional measurement ratio, defined by Tang, analyzes fibular rotation around the tibial centroid [23,26,29,40]. Measurements are depicted in Figure 3A–C and described in Table 1.

The orientation of the fibula within an uninjured syndesmosis has been described in relative detail in the currently available literature [5,13,20,22,28,29,31,33,36]. When imaged via CT, a mean internal rotation of 13.6° is observed in non-weight-bearing conditions, as opposed to 12.3° under weight-bearing conditions. Therefore, the fibula is exposed to an average 1.3° of external rotation when loaded. Fewer studies are available in the field of syndesmotic lesions. A mean external rotation of 7.61° was observed when comparing CT and WBCT. Furthermore, interobserver reliability was good in both non-weight-bearing (ICC = 0.689) and weight-bearing (ICC = 0.783) conditions. The reviewed studies reported no significant differences for age or sex, except for Wong et al., who noticed a naturally significant increase in internal rotation of 0.2° per year [31].

The bimalleolar angle was ascribed by two studies at different heights on axial CT images. Nault et al. measured the level of the talar dome, whereas Vetter et al. suggest that the ideal plane is located 4–6 mm more distal [28,37]. An average external rotation of 7.67° was achieved despite varying measurement heights. Good reliability was outlined by both authors (ICC = 0.68).

Just a handful of studies examined fibular rotation ratios, all within healthy syndesmosis populations [5,20,23,26,28,29]. A mean Tang ratio of 0.85 was found for both CT and WBCT. The corresponding ICC values are poor (ICC = 0.47) and good (ICC = 0.79), respectively. As for ratio A/B, a mean of 0.55 was found for CT and 0.62 for WBCT, thus resulting in a 0.07 increase of the external rotation when loaded. A good ICC was found in both CT (ICC = 0.72) and WBCT (ICC = 0.79).

3.3.2. The 2D Measurements Quantifying Syndesmotic Area

Despite numerous linear measurements, Malhotra et al. first described the area between the fibula and tibia 1 cm above the tibial plafond, i.e., the syndesmotic area, as depicted in Figure 2C and described in Table 1 [35]. Subsequently, this measure has been used increasingly. Multiple articles describe injured and uninjured syndesmoses in both non-weight-bearing and weight-bearing conditions [13,26,31,33–35].

Within healthy syndesmoses, a mean area of 105.2 mm^2 and 106 mm^2 was found for CT and WBCT, respectively. In the presence of lesions, the area increases to 129.5 mm^2 on CT and 134.1 mm^2 on WBCT. Therefore, injured syndesmoses are, on average, 24.3 mm^2 (CT) and 28.1 mm^2 (WBCT) larger compared to non-injured.

Hagemeijer et al. examined one cohort of unilateral injured and contralateral healthy syndesmoses in addition to a second cohort of bilateral uninjured ankles. Merely a mean difference of 0.41 mm² was detected between the left and right normal syndesmotoc areas, in contrast to a difference of 46 mm² of unilateral injury. These findings support the use of contralateral, uninjured syndesmosis as an internal control for injury assessment [33].

A significantly greater area ($p < 0.001$) was identified on CT images in injured ankles relative to normal ones [26,34,35]. Similar significance ($p < 0.001$) was achieved for WBCT [26,34]. Del Rio et al. reported a mean increase in the syndesmotoc area of 8.8% and 19.9% for CT and WBCT, respectively [34]. In addition, a larger area difference was detected between non-injured syndesmosis for men compared to women, which approached near significance for CT ($p = 0.069$) and WBCT ($p = 0.063$) [31,34]. Furthermore, weight-bearing induced a difference between normal and injured ankles that was significantly greater for men ($p = 0.04$) [34]. Wong et al. investigated the impact of a talocrural range of motion (ROM) on the syndesmotoc area and found that the surface decreased on average by 26 mm² ($p < 0.001$) going from dorsiflexion to plantar flexion [31].

Excellent interobserver reliability was documented for syndesmotoc area estimation for both CT (ICC = 0.96) and WBCT (ICC = 0.93).

3.4. Novel 3D Measurement Methods

Several studies have focused on transforming the aforementioned 2D measurements into a 3D framework. Several emerging 3D techniques have been found in the literature, which will be topically described below.

3.4.1. 3D Mirroring—Alignment Techniques

By mirroring the healthy and injured ankle in bilateral imaging, the contralateral ankle is used as internal control. After aligning both tibiae, the relative displacement of one fibula with respect to the control can be visualized and quantified (Figure 5). Ebinger et al. were the first to align both tibiae in a cadaveric study to quantify the 3D displacement of the fibula [23]. In their study, they have shown that 2D clinical measurements correlate poorly with the actual 3D displacement. Burssens et al. improved upon this using the contralateral healthy ankle as a template after mirroring the injured ankle to diagnose high ankle sprains and fracture-associated syndesmotoc lesions [3]. In their study, the average mediolateral diastasis of both the sprained group (mean = 1.6 mm) and the fracture group (mean = 1.7 mm) exhibited significant differences compared to the control group ($p < 0.001$). Additionally, they found a significant difference in the average external rotation between the sprained group (mean = 4.7°) and the fracture group (mean = 7.0°) when compared to the control group ($p < 0.05$). Peiffer et al. refined the examination of subtle syndesmotoc lesions using external torque during WBCT [41]. Significance was proven for ATFW and alpha angle computed on patient-specific 3D models.

3.4.2. The 3D Distance Mapping

Recently, the calculation of 3D distance maps has been introduced in ankle syndesmosis. These maps assess the relative position between two surfaces at each point, plotted on the bony contour. They are defined and calculated as the shortest surface-to-surface distance between each point of the 3D model and the opposing surface. Dibbern et al. were the first to apply these distance maps to the clinical entity of the syndesmosis [42]. The benefit of this technique is that it allows for an accurate and straightforward interpretation of the 3D tibiofibular diastasis in one image. In Figure 6, we have presented an example of distance mapping in a patient with a syndesmotoc injury.

3.4.3. The 3D Volume Measurements

Several authors have investigated the use of volumetric measurements of the distal tibiofibular articulation. In this technique, the total interosseous volume is calculated, extending from the level of the tibial plafond up to a height of 1, 3, 5, or 10 cm proximally (Figure 7). These 3D volume measurements were introduced by Taser et al. in their cadaveric experiment, showing a 43% (441 mm³) increase in syndesmotoc volume after 1 mm diastasis and an additional 20% increase for each extra 1 mm [43]. Ten years later, Kocadal et al. described the use of volume measurements to compare the post-operative syndesmotoc reduction between screw fixation and suture-button techniques, unveiling a significant increase of 8% (118.5 mm³) in suture-button fixation [44]. Additionally, they found an intra-observer reliability of 0.882 and an interobserver reliability of 0.861 for their measurement technique. Bhimani et al. and Ashkani-Esfahani et al. recently popularized these 3D volume measurements, showing high sensitivity (95.8%) and specificity (83.3%) for the detection of syndesmotoc instability [8,9]. Moreover, they stated a cut-off value of 11.6 cm³ (or 25.4% increase in volume) at the level of 5 cm above the tibial plafond, which reported an excellent ICC of 0.93.

3.4.4. The 3D Statistical Shape Model—Based Techniques

Peiffer et al. focused on using statistical shape models and ligament modeling techniques to model the path and quantify the predicted length of the syndesmotoc ligaments in patients with high ankle sprains and asymptomatic controls [17]. They reported a statistically significant difference in anterior tibiofibular ligament length between ankles with syndesmotoc lesions and healthy controls ($p = 0.017$). They also found a significant correlation between the presence of syndesmotoc injury and the positional alignment between the distal tibia and fibula ($r = 0.873$, $p < 0.001$). More specifically, they described an “anterior open-book injury” of the ankle syndesmosis as a result of anterior inferior tibiofibular ligament elongation/rupture (Figure 8).

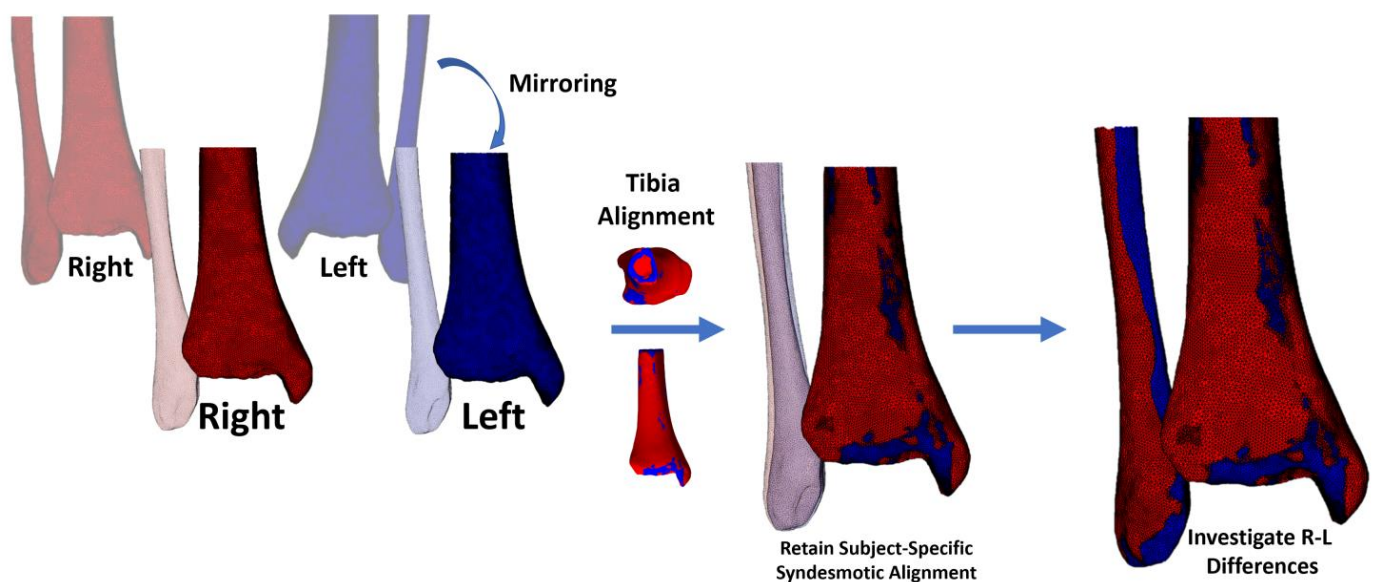


Figure 5. Mirroring and alignment of the right (red) and left (blue) ankle. The left ankle tibia is mirrored and rigidly registered to the right tibia. By aligning both tibiae, the side-specific anatomical configuration of the ankle syndesmosis is retained, and the relative displacement of the fibula can be visualized.

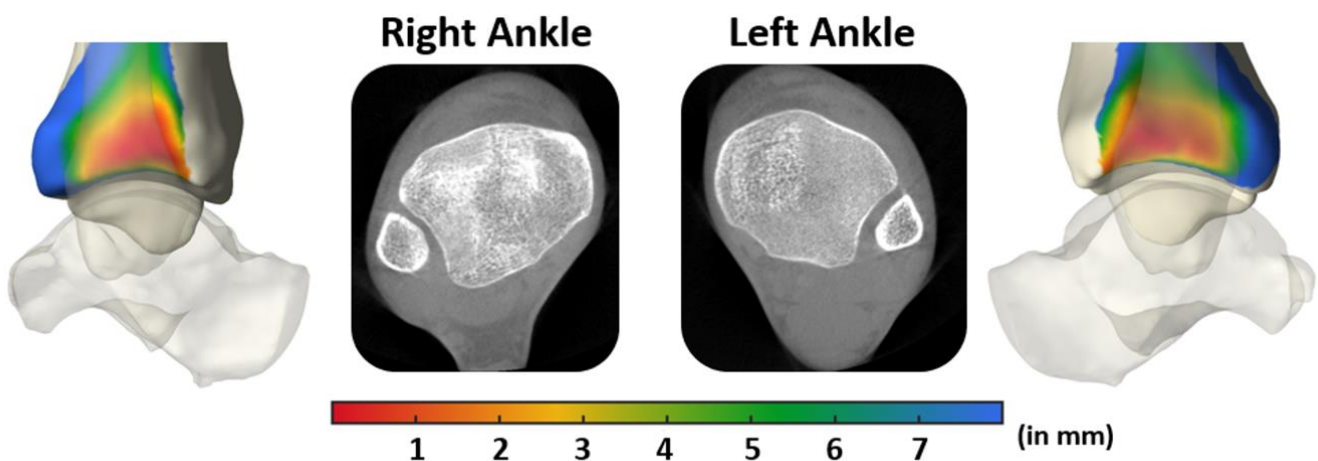


Figure 6. Example of distance map analysis. Weight-bearing CT images in a patient with a syndesmotic injury in the left ankle. A corresponding 3D distance mapping is presented, which reveals an increased tibiofibular clear space on the left side.

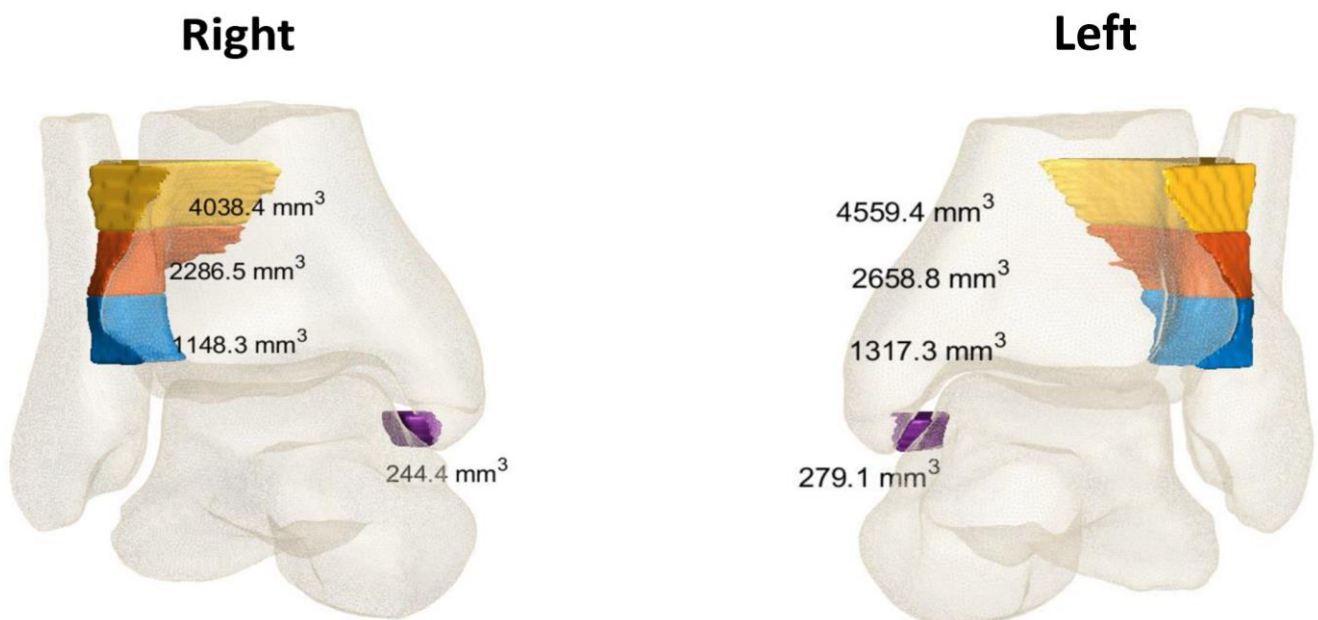


Figure 7. Volumetric measurements of the **right** and **left** distal tibiofibular joint (up to 1, 2, and 3 cm) and medial gutter in a patient with **left** Weber-B fracture using Disior™ (Paragon 28®, Bonellogic F&A).

3.4.5. Other Novel Measurement Techniques

More recently, a study explored the use of dual-energy CT post-processing algorithms [45]. More specifically, they looked at the accuracy of collagen mapping technology compared to grayscale CT analysis in the assessment of syndesmotic integrity. The results showed that collagen mapping significantly enhanced sensitivity, specificity, positive predictive value, negative predictive value, and overall accuracy for detecting distal tibiofibular syndesmosis injuries. Additionally, collagen mapping achieved higher diagnostic confidence, image quality, and noise scores compared to grayscale CT.

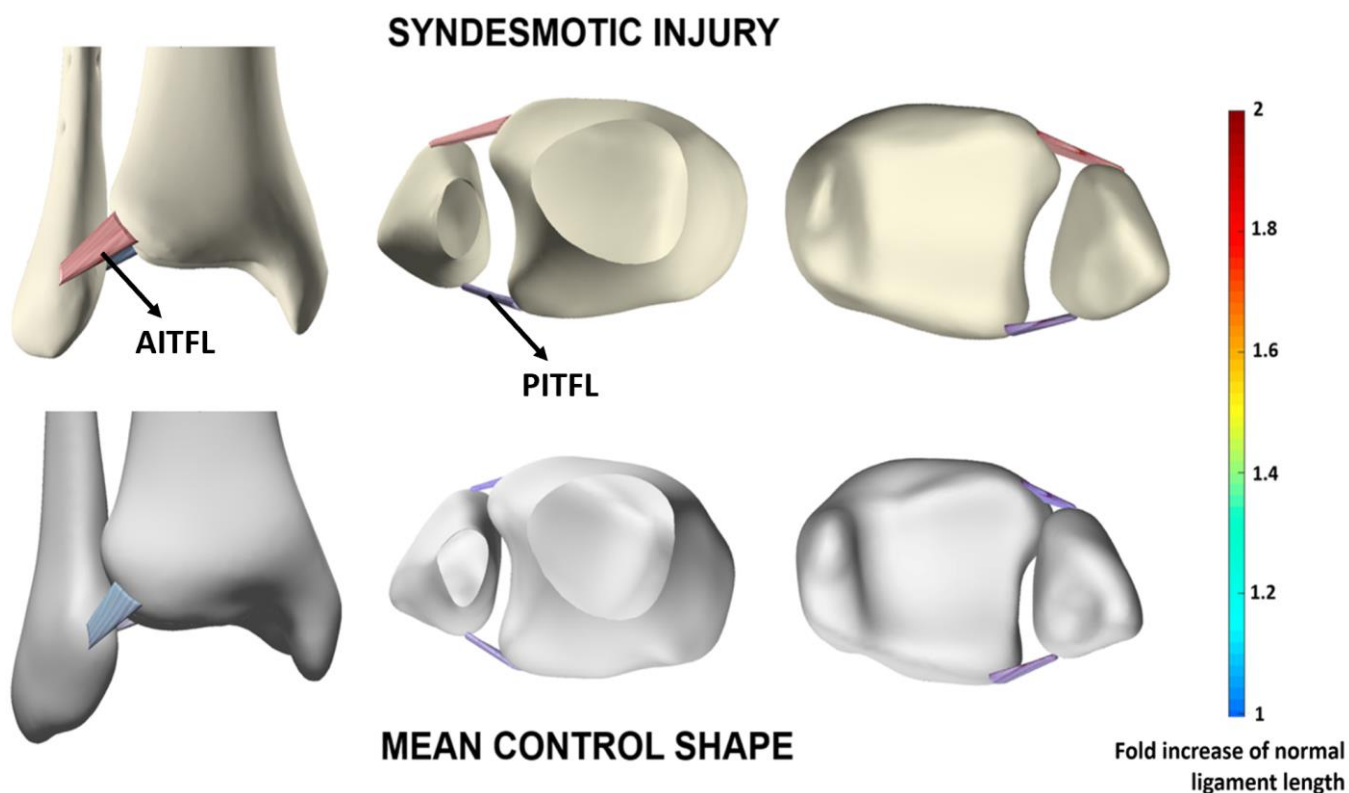


Figure 8. Distal tibiofibular joint anatomy in a documented syndesmotic lesion (**top**) versus the mean control distal tibiofibular joint anatomy, derived from a statistical shape model (**bottom**). The statistical shape model-based ligament modeling framework was able to detect an increase of anterior inferior tibiofibular ligament distance by 170%, resulting in an anterior “open-book” injury.

4. Discussion

A broad set of measurements exists to evaluate syndesmotic integrity [46]. However, these measurements are scattered across the literature. Therefore, this topical review compiled the current evidence available in the literature, with the aim of providing a comprehensive overview of which 2D/3D measurements are at hand. No systematic review was obtained because of the heterogeneity of the trials. This made it difficult to compare the results of the trials. Secondly, the aim was to look at newer and emerging techniques. These are usually described in individual trials, so a systematic review was not possible. Although the majority of ICC values for 2D measurements indicate high reliability, specific measurements that involve multiple steps show lower ICC values, likely due to the learning curve. The 3D measurement techniques are emerging as promising alternatives and could replace 2D measurements in the future, but they have not yet been integrated into daily clinical practice.

Regarding 2D measurements, there are several techniques to quantify mediolateral translation, anteroposterior translation, rotation, and area. The mediolateral tibiofibular translation measurements were the most commonly used [5,6,13,18,20,22–32]. Interobserver reliability was good to excellent for all measurements. There was also no significant difference between bilateral ankles, which can be compared to assess syndesmotic integrity [6,31]. No studies have shown a significant increase in width between non-weight-bearing and weight-bearing conditions, but the average of the means was greater in weight-bearing conditions for each measurement [20,29]. Greater distances have been shown for each measurement when comparing normal and injured ankles in non-weight-bearing conditions. In weight-bearing conditions, only a significant difference has been shown for one mediolateral translation measurement: MTFW [22,26,32,33,47]. Studies have reported cut-off values for ATFW, MTFW, and MxTFW with varying sensitivity and specificity [5,18,32]. For each

measure, there are studies that demonstrate that the measure is adequate to discriminate between normal and injured ankles, but more research is needed to formulate a consensus on cut-off values.

The anteroposterior translation of the fibula relative to the tibia can be assessed using two commonly used measurements [5,28,38]. The anterior Phisitkul is the most commonly used translational parameter [5,13,20,23,26,28,29,38,39]. Unfortunately, most studies only include normal ankles, and just one study evaluated injured ankles in both non-weight-bearing and weight-bearing conditions [39]. An excellent AUC value was achieved in non-weight-bearing conditions (0.894), suggesting that the anterior Phisitkul could be an excellent parameter in the diagnosis of syndesmotic injuries [26]. Nault's translational parameter is an interesting method but is only used in three studies with normal ankles [5,20,28]. Comparative studies are needed to assess whether this parameter can be used in the diagnosis of syndesmotic injury. Other studies have also described measurements of anteroposterior translation, but as these measurements were rarely used and lacked validation, they were not discussed in this review [26,27,33].

The main rotation measurements were the fibular rotation parameter by Dikos et al. [34]. With respect to this measurement, our findings suggest that the mean rotation of the fibula under weight-bearing conditions was 12.3° internal rotation, as compared to 7.39° in the presence of lesions. A lesser-used rotational parameter, the bimalleolar angle, has been suggested by Vetter et al. as a valid alternative, given its simpler methodology with clear anatomical landmarks. The measurement is made at a talocrural level, which could potentially be advantageous in the evaluation of fractures and dislocations [37]. Moreover, ratios describing the fibular rotations have been infrequently reported. A possible explanation could be the complexity and inherent errors associated with these measurements [5].

The syndesmotic area exhibited a significant increase in injured syndesmoses, as observed in both CT and WBCT scans, in comparison to non-injured cases [13,26,31,33–35]. The difference in the area under weight-bearing conditions was notably larger, with an additional 3.8 mm² [31,34]. Notably, the syndesmotic area demonstrated particularly high ICC values of 0.96 for CT and 0.93 for WBCT, surpassing other measurements. These findings emphasize the validity of the syndesmotic area as the currently most reliable parameter available.

Regarding 3D Measurements, we found a broad set of novel techniques to circumvent the flaws of 2D measurement techniques. Particularly, distance mapping and volumetric analysis have shown great potential to increase the inter- and intra-observer reliability and automate the measurement process. The ICC of these volume measurements has increased up to 0.93, while distance mapping measurements have been performed fully automated, eliminating all observer inaccuracies [8,9,42–44].

This review demonstrates that despite the existence of numerous studies investigating syndesmotic measurements on CT scans, a definitive consensus regarding the appropriate measurements for assessing syndesmotic integrity is still lacking. Multiple measurements have been described, each varying in complexity, which creates difficulty in discerning the most reliable approaches. While most ICC values indicate good to excellent reliability, certain measurements involving multiple steps exhibit lower ICC values, likely due to the learning curve associated with their implementation. Findings regarding the influence of age, sex, and height on syndesmotic measurements are inconclusive, but there is no significant difference observed between bilateral ankles, allowing for the comparison to the opposite side as an internal control. There is a considerable range of normal and pathological values, as evidenced by the standard deviation associated with each measurement. Taken together, these factors contribute to the challenge of distinguishing between normal and pathological values in routine clinical practice.

Several limitations should be noted in this review. Firstly, many studies have small sample sizes. In addition, this review includes a diverse group of studies, and not all studies include patients with a syndesmotic injury. Additionally, it was difficult to make direct comparisons between every injury group due to variations in the nature of the injuries.

Furthermore, it is difficult to draw conclusions about the diagnostic accuracy of CT and WBCT as most of the studies looked at normal syndesmotic anatomy. As a result, it is evidently difficult to establish cut-off values. Studies with larger sample sizes, including more patients with syndesmotic injuries, could further clarify the remaining questions about the diagnostic accuracy of CT and WBCT measurements.

Future Perspectives

Future studies should continue to examine the merits of WBCT over CT to diagnose (subtle) syndesmotic lesions, preferably in a (semi-)automated manner [48]. Larger populations of injured versus healthy individuals should be analyzed. The implementation of external rotation stress during WBCT needs to be validated as a potential enhancer for the detection of lesions. The emergence of 3D techniques requires further exploration, whether in terms of distance, area, or volume measures. In clinical practice, cut-off values for both 2D and 3D measurements are necessary to improve lesion diagnosis and correlate these with therapy strategies.

5. Conclusions

In this review, we have topically described the available 2D and 3D measurements to assess and quantify syndesmotic integrity. While most ICC values of 2D measurements indicate good to excellent reliability, certain measurements involving multiple steps exhibit lower ICC values, likely due to the learning curve. The 3D measurement techniques are emerging as encouraging alternatives but are not implemented yet in daily clinical practice.

Author Contributions: Conceptualization, M.P. and A.B.; methodology, T.D. and M.H.; software, T.D. and M.H.; formal analysis, T.D. and M.H.; investigation, T.D., M.H. and M.P.; resources, T.D. and M.H.; data curation, T.D. and M.H.; writing—original draft preparation, T.D. and M.H.; writing—review and editing, M.P., B.K., N.H., N.K. and E.A.; visualization, T.D., M.H. and M.P.; supervision, E.A. and A.B.; project administration, M.P. All authors have read and agreed to the published version of the manuscript.

Funding: This research received no external funding.

Institutional Review Board Statement: Not applicable.

Informed Consent Statement: Not applicable.

Data Availability Statement: Data sharing not applicable. No new data were created or analyzed in this study. Data sharing is not applicable to this article.

Conflicts of Interest: The authors declare no conflict of interest.

References

1. Campbell, S.E.; Warner, M. MR Imaging of Ankle Inversion Injuries. *Magn. Reson. Imaging Clin. N. Am.* **2008**, *16*, 1–18. [[CrossRef](#)] [[PubMed](#)]
2. Chans-Veres, J.; Vallejo-Márquez, M.; Galhoum, A.E.; Tejero, S. Analysis of the uninjured tibiofibular syndesmosis using conventional CT-imaging and axial force in different foot positions. *Foot Ankle Surg.* **2022**, *28*, 650–656. [[CrossRef](#)] [[PubMed](#)]
3. Burssens, A.; Vermue, H.; Barg, A.; Krähenbühl, N.; Victor, J.; Buedts, K. Templating of Syndesmotic Ankle Lesions by Use of 3D Analysis in Weightbearing and Nonweightbearing CT. *Foot Ankle Int.* **2018**, *39*, 1487–1496. [[CrossRef](#)] [[PubMed](#)]
4. Chun, D.-I.; Cho, J.-H.; Min, T.-H.; Yi, Y.; Park, S.Y.; Kim, K.-H.; Kim, J.H.; Won, S.H. Diagnostic accuracy of radiologic methods for ankle syndesmosis injury: A systematic review and meta-analysis. *J. Clin. Med.* **2019**, *8*, 968. [[CrossRef](#)] [[PubMed](#)]
5. Patel, S.; Malhotra, K.; Cullen, N.P.; Singh, D.; Goldberg, A.J.; Welck, M.J. Defining reference values for the normal tibiofibular syndesmosis in adults using weight-bearing CT. *Bone Jt. J.* **2019**, *101-B*, 348–352. [[CrossRef](#)] [[PubMed](#)]
6. Park, C.H.; Kim, G.B. Tibiofibular relationships of the normal syndesmosis differ by age on axial computed tomography—Anterior fibular translation with age. *Injury* **2019**, *50*, 1256–1260. [[CrossRef](#)] [[PubMed](#)]
7. Ng, N.; Onggo, J.R.; Nambiar, M.; Maingard, J.T.; Ng, D.; Gupta, G.; Nandurkar, D.; Babazadeh, S.; Bedi, H. Which test is the best? An updated literature review of imaging modalities for acute ankle diastasis injuries. *J. Med. Radiat. Sci.* **2022**, *69*, 382–393. [[CrossRef](#)]
8. Esfahani, S.A.; Bhimani, R.; Lubberts, B.; Kerkhoffs, G.M.; Waryasz, G.; DiGiovanni, C.W.; Guss, D. Volume measurements on weightbearing computed tomography can detect subtle syndesmotic instability. *J. Orthop. Res.* **2022**, *40*, 460–467. [[CrossRef](#)]

9. Bhimani, R.; Ashkani-Esfahani, S.; Lubberts, B.; Guss, D.; Hagemeyer, N.C.; Waryasz, G.; DiGiovanni, C.W. Utility of Volumetric Measurement via Weight-Bearing Computed Tomography Scan to Diagnose Syndesmotic Instability. *Foot Ankle Int.* **2020**, *41*, 859–865. [[CrossRef](#)]
10. Campbell, T.; Mok, A.; Wolf, M.R.; Tarakemeh, A.; Everist, B.; Vopat, B.G. Augmented stress weightbearing CT for evaluation of subtle tibiofibular syndesmotic injuries in the elite athlete. *Skelet. Radiol.* **2022**, *52*, 1221–1227. [[CrossRef](#)]
11. Sman, A.D.; Hiller, C.E.; Rae, K.; Linklater, J.; Black, D.A.; Nicholson, L.L.; Burns, J.; Refshauge, K.M. Diagnostic accuracy of clinical tests for ankle syndesmosis injury. *Br. J. Sports Med.* **2015**, *49*, 323–329. [[CrossRef](#)] [[PubMed](#)]
12. Baltes, T.P.A.; Al Sayrafi, O.; Arnáiz, J.; Al-Naimi, M.R.; Geertsema, C.; Geertsema, L.; Holtzhausen, L.; D’hooghe, P.; Kerkhoffs, G.M.M.J.; Tol, J.L. Acute clinical evaluation for syndesmosis injury has high diagnostic value. *Knee Surg. Sports Traumatol. Arthrosc.* **2022**, *30*, 3871–3880. [[CrossRef](#)] [[PubMed](#)]
13. Abdelaziz, M.E.; Hagemeyer, N.; Guss, D.; El-Hawary, A.; El-Mowafi, H.; DiGiovanni, C.W. Evaluation of Syndesmosis Reduction on CT Scan. *Foot Ankle Int.* **2019**, *40*, 1087–1093. [[CrossRef](#)] [[PubMed](#)]
14. Anand Prakash, D.A. Syndesmotic stability: Is there a radiological normal?—A systematic review. *Foot Ankle Surg.* **2018**, *24*, 174–184. [[CrossRef](#)] [[PubMed](#)]
15. Chang, A.L.; Mandell, J.C. Syndesmotic Ligaments of the Ankle: Anatomy, Multimodality Imaging, and Patterns of Injury. *Curr. Probl. Diagn. Radiol.* **2020**, *49*, 452–459. [[CrossRef](#)] [[PubMed](#)]
16. Krähenbühl, N.; Akkaya, M.; Dodd, A.E.; Hintermann, B.; Dutilh, G.; Lenz, A.L.; Barg, A. Impact of the rotational position of the hindfoot on measurements assessing the integrity of the distal tibio-fibular syndesmosis. *Foot Ankle Surg.* **2020**, *26*, 810–817. [[CrossRef](#)] [[PubMed](#)]
17. Peiffer, M.; Burssens, A.; De Mits, S.; Heintz, T.; Van Waeyenberge, M.; Buedts, K.; Victor, J.; Audenaert, E. Statistical shape model-based tibiofibular assessment of syndesmotic ankle lesions using weight-bearing CT. *J. Orthop. Res.* **2022**, *40*, 2873–2884. [[CrossRef](#)]
18. Rodrigues, J.C.; do Amaral e Castro, A.; Rosemberg, L.A.; de Cesar Netto, C.; Godoy-Santos, A.L. Diagnostic Accuracy of Conventional Ankle CT Scan with External Rotation and Dorsiflexion in Patients with Acute Isolated Syndesmotic Instability. *Am. J. Sports Med.* **2023**, *51*, 985–996. [[CrossRef](#)]
19. Wohlin, C. Guidelines for snowballing in systematic literature studies and a replication in software engineering. In Proceedings of the 18th International Conference on Evaluation and Assessment in Software Engineering, London, UK, 13–14 May 2014; ACM: New York, NY, USA, 2014; pp. 1–10. [[CrossRef](#)]
20. Malhotra, K.; Welck, M.; Cullen, N.; Singh, D.; Goldberg, A.J. The effects of weight bearing on the distal tibiofibular syndesmosis: A study comparing weight bearing-CT with conventional CT. *Foot Ankle Surg.* **2019**, *25*, 511–516. [[CrossRef](#)]
21. Page, M.J.; McKenzie, J.E.; Bossuyt, P.M.; Boutron, I.; Hoffmann, T.C.; Mulrow, C.D.; Shamseer, L.; Tetzlaff, J.M.; Akl, E.A.; Brennan, S.E.; et al. The PRISMA 2020 statement: An updated guideline for reporting systematic reviews. *BMJ* **2021**, *372*, n71. [[CrossRef](#)]
22. Ahn, T.K.; Choi, S.M.; Kim, J.Y.; Lee, W.C. Isolated Syndesmosis Diastasis: Computed Tomography Scan Assessment with Arthroscopic Correlation. *Arthrosc. J. Arthrosc. Relat. Surg.* **2017**, *33*, 828–834. [[CrossRef](#)] [[PubMed](#)]
23. Ebinger, T.; Goetz, J.; Dolan, L.; Phisitkul, P. 3D Model analysis of existing CT syndesmosis measurements. *Iowa Orthop. J.* **2013**, *33*, 40–46. [[PubMed](#)]
24. Elgafy, H.; Semaan, H.B.; Blessinger, B.; Wassef, A.; Ebraheim, N.A. Computed tomography of normal distal tibiofibular syndesmosis. *Skelet. Radiol.* **2010**, *39*, 559–564. [[CrossRef](#)] [[PubMed](#)]
25. Gardner, M.J.; Demetrakopoulos, D.; Briggs, S.M.; Helfet, D.L.; Lorich, D.G. Malreduction of the Tibiofibular Syndesmosis in Ankle Fractures. *Foot Ankle Int.* **2006**, *27*, 788–792. [[CrossRef](#)] [[PubMed](#)]
26. Hamard, M.; Neroladaki, A.; Bagetakos, I.; Dubois-Ferrière, V.; Montet, X.; Boudabbous, S. Accuracy of cone-beam computed tomography for syndesmosis injury diagnosis compared to conventional computed tomography. *Foot Ankle Surg.* **2020**, *26*, 265–272. [[CrossRef](#)] [[PubMed](#)]
27. Lepojärvi, S.; Niinimäki, J.; Pakarinen, H.; Leskelä, H.V. Rotational Dynamics of the Normal Distal Tibiofibular Joint with Weight-Bearing Computed Tomography. *Foot Ankle Int.* **2016**, *37*, 627–635. [[CrossRef](#)] [[PubMed](#)]
28. Nault, M.-L.; Hébert-Davies, J.; Laflamme, G.-Y.; Leduc, S. CT Scan Assessment of the Syndesmosis: A New Reproducible Method. *J. Orthop. Trauma.* **2013**, *27*, 638–641. [[CrossRef](#)]
29. Shakoob, D.; Osgood, G.M.; Brehler, M.; Zbijewski, W.B.; Netto, C.d.C.; Shafiq, B.; Orapin, J.; Thawait, G.K.; Shon, L.C.; Demehri, S. Cone-beam CT measurements of distal tibio-fibular syndesmosis in asymptomatic uninjured ankles: Does weight-bearing matter? *Skelet. Radiol.* **2019**, *48*, 583–594. [[CrossRef](#)]
30. Wong, F.; Mills, R.; Mushtaq, N.; Walker, R.; Singh, S.K.; Abbasian, A. Correlation and comparison of syndesmosis dimension on CT and MRI. *Foot* **2016**, *28*, 36–41. [[CrossRef](#)]
31. Wong, M.T.; Wiens, C.; Lamothe, J.; Edwards, W.B.; Schneider, P.S. Four-Dimensional CT Analysis of Normal Syndesmotic Motion. *Foot Ankle Int.* **2021**, *42*, 1491–1501. [[CrossRef](#)]
32. Yeung, T.W.; Chan, C.Y.G.; Chan, W.C.S.; Yeung, Y.N.; Yuen, M.K. Can pre-operative axial CT imaging predict syndesmosis instability in patients sustaining ankle fractures? Seven years’ experience in a tertiary trauma center. *Skelet. Radiol.* **2015**, *44*, 823–829. [[CrossRef](#)] [[PubMed](#)]

33. Hagemeyer, N.C.; Chang, S.H.; Abdelaziz, M.E.; Casey, J.C.; Waryasz, G.R.; Guss, D.; DiGiovanni, C.W. Range of Normal and Abnormal Syndesmotic Measurements Using Weightbearing CT. *Foot Ankle Int.* **2019**, *40*, 1430–1437. [[CrossRef](#)] [[PubMed](#)]
34. del Rio, A.; Bewsher, S.M.; Roshan-Zamir, S.; Tate, J.; Eden, M.; Gotmaker, R.; Wang, O.; Bedi, H.S.; Rotstein, A.H. Weightbearing Cone-Beam Computed Tomography of Acute Ankle Syndesmosis Injuries. *J. Foot Ankle Surg.* **2020**, *59*, 258–263. [[CrossRef](#)] [[PubMed](#)]
35. Malhotra, G.; Cameron, J.; Toolan, B.C. Diagnosing chronic diastasis of the syndesmosis: A novel measurement using computed tomography. *Foot Ankle Int.* **2014**, *35*, 483–488. [[CrossRef](#)] [[PubMed](#)]
36. Dikos, G.D.; Heisler, J.; Choplin, R.H.; Weber, T.G. Normal Tibiofibular Relationships at the Syndesmosis on Axial CT Imaging. *J. Orthop. Trauma.* **2012**, *26*, 433–438. [[CrossRef](#)] [[PubMed](#)]
37. Vetter, S.Y.; Gassauer, M.; Uhlmann, L.; Swartman, B.; Schnetzke, M.; Keil, H.; Franke, J.; Grützner, P.A.; Beisemann, N. A standardised computed tomography measurement method for distal fibular rotation. *Eur. J. Trauma. Emerg. Surg.* **2021**, *47*, 891–896. [[CrossRef](#)] [[PubMed](#)]
38. Phisitkul, P.; Ebinger, T.; Goetz, J.; Vaseenon, T.; Marsh, J.L. Forceps reduction of the syndesmosis in rotational ankle fractures: A cadaveric study. *J. Bone Joint Surg. Am.* **2012**, *94*, 2256–2261. [[CrossRef](#)] [[PubMed](#)]
39. Osgood, G.M.; Shakoor, D.; Orapin, J.; Qin, J.; Khodarahmi, I.; Thawait, G.K.; Ficke, J.R.; Schon, L.C.; Demehri, S. Reliability of distal tibio-fibular syndesmotic instability measurements using weightbearing and non-weightbearing cone-beam CT. *Foot Ankle Surg.* **2019**, *25*, 771–781. [[CrossRef](#)]
40. Tang, C.W.; Roidis, N.; Vaishnav, S.; Patel, A.; Thordarson, D.B. Position of the Distal Fibular Fragment in Pronation and Supination Ankle Fractures: A CT Evaluation. *Foot Ankle Int.* **2003**, *24*, 561–566. [[CrossRef](#)]
41. Peiffer, M.; Dhont, T.; Cuigniez, F.; Tampere, T.; Ashkani-Esfahani, S.; D’hooghe, P.; Audenaert, E.; Burssens, A. Application of external torque enhances the detection of subtle syndesmotic ankle instability in a weight-bearing CT. *Knee Surg. Sports Traumatol. Arthrosc.* **2023**; *Online ahead of print.* [[CrossRef](#)]
42. Dibbern, K.; Vivtcharenko, V.; Mansur, N.S.B.; Lalevée, M.; de Carvalho, K.A.M.; Lintz, F.; Barg, A.; Goldberg, A.J.; Netto, C.d.C. Distance mapping and volumetric assessment of the ankle and syndesmotic joints in progressive collapsing foot deformity. *Sci. Rep.* **2023**, *13*, 4801. [[CrossRef](#)]
43. Taser, F.; Shafiq, Q.; Ebraheim, N.A. Three-dimensional volume rendering of tibiofibular joint space and quantitative analysis of change in volume due to tibiofibular syndesmosis diastases. *Skelet. Radiol.* **2006**, *35*, 935–941. [[CrossRef](#)] [[PubMed](#)]
44. Kocadal, O.; Yucel, M.; Pepe, M.; Aksahin, E.; Aktekin, C.N. Evaluation of Reduction Accuracy of Suture-Button and Screw Fixation Techniques for Syndesmotic Injuries. *Foot Ankle Int.* **2016**, *37*, 1317–1325. [[CrossRef](#)] [[PubMed](#)]
45. Gruenewald, L.D.; Leitner, D.H.; Koch, V.; Martin, S.S.; Yel, I.; Mahmoudi, S.; Bernatz, S.; Eichler, K.; Gruber-Rouh, T.; Dos Santos, D.P.; et al. Diagnostic Value of DECT-Based Collagen Mapping for Assessing the Distal Tibiofibular Syndesmosis in Patients with Acute Trauma. *Diagnostics* **2023**, *13*, 533. [[CrossRef](#)] [[PubMed](#)]
46. Krähenbühl, N.; Weinberg, M.W.; Davidson, N.P.; Mills, M.K.; Hintermann, B.; Saltzman, C.L.; Barg, A. Imaging in syndesmotic injury: A systematic literature review. *Skelet. Radiol.* **2018**, *47*, 631–648. [[CrossRef](#)] [[PubMed](#)]
47. Rodrigues, J.C.; Santos, A.L.G.; Prado, M.P.; Alloza, J.F.M.; Masagão, R.A.; Rosemberg, L.A.; Barros, D.D.C.S.; e Castro, A.D.A.; Demange, M.K.; Lenza, M.; et al. Comparative CT with stress manoeuvres for diagnosing distal isolated tibiofibular syndesmotic injury in acute ankle sprain: A protocol for an accuracy-test prospective study. *BMJ Open* **2020**, *10*, e037239. [[CrossRef](#)] [[PubMed](#)]
48. Peiffer, M.; Van Den Borre, I.; Segers, T.; Ashkani-Esfahani, S.; Guss, D.; De Cesar Netto, C.; DiGiovanni, C.W.; Victor, J.; Audenaert, E. Implementing automated 3D measurements to quantify reference values and side-to-side differences in the ankle syndesmosis. *Sci. Rep.* **2023**, *13*, 13774. [[CrossRef](#)]

Disclaimer/Publisher’s Note: The statements, opinions and data contained in all publications are solely those of the individual author(s) and contributor(s) and not of MDPI and/or the editor(s). MDPI and/or the editor(s) disclaim responsibility for any injury to people or property resulting from any ideas, methods, instructions or products referred to in the content.